

## MATERIAL AND METHODS

### Preparation of Unloaded Doxil Liposomes

Doxil liposomes were prepared by the lipid film hydration and extrusion method (1). A mixture containing hydrogenated soy phosphatidylcholine (HSPC; Lipoid GmbH, Ludwigshaven, Germany), cholesterol (Sigma-Aldrich, Zwijndrecht, the Netherlands), 1,2-distearoyl-*sn*-glycerol-3-phosphoethanolamine-N-[methoxy(polyethylene glycol)-2000] (ammonium salt) (18:0 PEG2000 PE; Lipoid GmbH), 1,2-distearoyl-*sn*-glycerol-3-phosphoethanolamine-N-diethylenetriaminepentaacetic acid (ammonium salt) (18:0 PE-DTPA; Avanti Polar lipids, Alabaster, AL) in a molar ratio 57:38:5:0.1 was dissolved in chloroform/methanol 9:1 (vol/vol). After the addition of 0.1 mol% 1,2-dipalmitoyl-*sn*-glycero-3-phosphoethanolamine-N-(lissamine rhodamine B sulfonyl) (ammonium salt) (Rhodamine-PE; Avanti Polar lipids), the solvent was evaporated *in vacuo* using a rotary evaporator (Büchi Rotavapor R-210, Büchi Labortechnik, Flawil, Switzerland) until a homogeneous lipid film was formed. The lipid film was hydrated in 4-(2-hydroxyethyl)-1-piperazineethanesulfonic acid (HEPES) buffered saline (10 mM HEPES, 135 mM NaCl, pH 7.4). The newly formed vesicles were extruded at 60°C through a high-pressure Lipex thermoline extruder (Northern Lipids Inc, Vancouver, Canada) by passing through Nucleopore polycarbonate membrane filters (Whatman, Newton, MA) with pore diameters of 200, 100, 80, and 50 nm (5 extrusions per filter). The average diameter and size distribution (polydispersity index) of the liposomes were determined by dynamic light scattering using a Zetasizer Nano (Malvern Instruments, Worcestershire, United Kingdom). Total phospholipid content was determined by phosphate assay, as described elsewhere (2).

### Cell Lines

Established human cell lines were used, among which: one squamous cell carcinoma cell line (A431), four pancreatic adenocarcinoma (AsPC-1, BxPC-3, CFPAC-1, HPAF-II), one epithelioid carcinoma (PANC-1), two breast adenocarcinoma (MDA-MB-231, MDA-MB-468), and one primary ductal breast carcinoma (UACC-893). Cell culture reagents were purchased from Lonza (Breda, the Netherlands). A431, CFPAC-1, and PANC-1 were grown in Dulbecco's Modified Eagle Medium with glutamine supplemented with 10% fetal bovine serum; AsPC-1, BxPC-3, MDA-MB-231, MDA-MB-468, and UACC-893 were grown in Roswell Park Memorial Institute 1640 medium supplemented with 10% fetal bovine serum; HPAF-II was grown in Roswell Park Memorial Institute 1640 medium with glutamine supplemented with 5% fetal bovine serum.

### **In Vivo Biodistribution Studies**

NMRI nu/nu mice were obtained from Harlan (Horst, the Netherlands). All experiments were performed according to the guidelines for research animals and approved by the Animal Welfare Committee of the Erasmus Medical Center. 9-week-old male NMRI (nu/nu) mice were injected subcutaneously in the right flank with  $3\text{-}5 \times 10^6$  cells in 100  $\mu\text{L}$  phosphate buffered saline. Mice were anesthetized with the inhalation anesthetic isoflurane during injection of cells and SPECT/CT imaging. Tumors were measured by caliper every other day till grown to an average size of 200  $\text{mm}^3$ . Tumor volumes were calculated using the formula:  $V = 0.4 * (a * b * c)$ , where  $a$ ,  $b$  and  $c$  represent the length, width and depth of the tumor, respectively.

### **Immunohistochemical Staining**

Harvested tumors were snap-frozen in liquid nitrogen and frozen tumor sections (10  $\mu\text{m}$  thick) were mounted on Superfrost++ slides (VWR, Radnor, PA). The slides were fixed with acetone at 4°C for 10 min and stained for the following morphological parameters: blood vessels (Rat-anti-

mouse CD31, 1:100; Becton Dickinson, Franklin Lakes, NJ), PEGylated liposomes (Rabbit-anti-PEG, 1:100; Abcam, Cambridge, United Kingdom), macrophages (Rat-anti-mouse CD11b, 1:100; eBioscience, San Diego, CA), lymphatic vessels (rabbit-anti-LYVE1, 1:100; Abcam) and vessel integrity (Rabbit-anti-Collagen IV, 1:100; Millipore, Billerica, MA). Hypoxia was detected with a rabbit-anti-pimonidazole antibody (1:200, Hypoxiprobe, Burlington, MA). Secondary antibodies were species-specific donkey-antibodies conjugated with AF488 or AF647 (1:500) (Molecular Probes, Waltham, MA) in appropriate combinations.

### **In Vitro Stability Assay**

Liposomes were made and radiolabeled with  $^{111}\text{In}$  as described before. These liposomes were incubated in 100% fetal bovine serum at 37°C for 24, 48, 72, 96 h. The solution was eluted over a size exclusion chromatography column (PD-10, GE Healthcare, Buckinghamshire, United Kingdom) and fractions of 1 mL were collected. After elution the column was washed with 25 mL phosphate buffered saline to check for free  $^{111}\text{In}$ -DTPA.

### **In Vivo Stability Assay**

Mice were injected with 1  $\mu\text{mol}$   $^{111}\text{In}$ -labeled liposomes and were followed over time. After 24 and 96 h the mice were used for biodistribution experiments as described before.

## RESULTS

### Characterization of Liposomes

Lipids and cholesterol were used in the ratio as described for preparing liposomes comparable to Doxil. The addition of cholesterol increases liposome stability in plasma and pegylation provides a long circulation half-life by creating a steric barrier against opsonization (3). Doxil is one of the few liposomal drugs approved for clinical use in breast cancer (4), ovarian cancer (5), multiple myeloma, and HIV-related Kaposi's sarcoma (6,7). The formulation used here was not loaded with doxorubicin, as the principal objective was to assess the distribution behavior of the liposomes *in vivo*. All other characteristics are similar to Doxil, such as an average size of  $83.13 \pm 2.69$  nm and polydispersity index of  $0.036 \pm 0.016$ .

### Tumor Characterization

After inoculation tumor volume was measured every other day until a size of 200-300 mm<sup>3</sup> was reached. Supplemental Figure 1 shows the growth rate of individual s.c. xenografts subdivided in groups of fast (Supplemental Figure 1A), intermediate (Supplemental Figure 1B), and slow growing xenografts (Supplemental Figure 1C). The squamous cell carcinoma A431, and pancreatic adenocarcinoma's CFPAC-1 and HPAF-II are fast growing tumors, which grew to the target size within 1 month. Pancreatic adenocarcinomas AsPC-1, BxPC-3, and breast adenocarcinoma MDA-MB-231 needed 1.5-2.5 months, whereas slow growing tumors, such as primary ductal carcinoma UACC-893, epithelioid carcinoma PANC-1, and breast adenocarcinoma MDA-MB-468 needed 3-6 months. With few exceptions (e.g. MDA-MB-231), the tumors showed a predictable and reproducible growth pattern. This subdivision was used to compare various parameters thought to be involved in the EPR effect and uptake of liposomes. Supplemental Table 1 shows an increased

liposomal uptake *in vivo* and *ex vivo*, in fast growing xenografts compared to slow growing xenografts ( $p < 0.01$ ). However, no other parameter could be clearly identified as being involved in liposomal uptake with this subdivision of xenografts.

### **In Vitro Stability Assay**

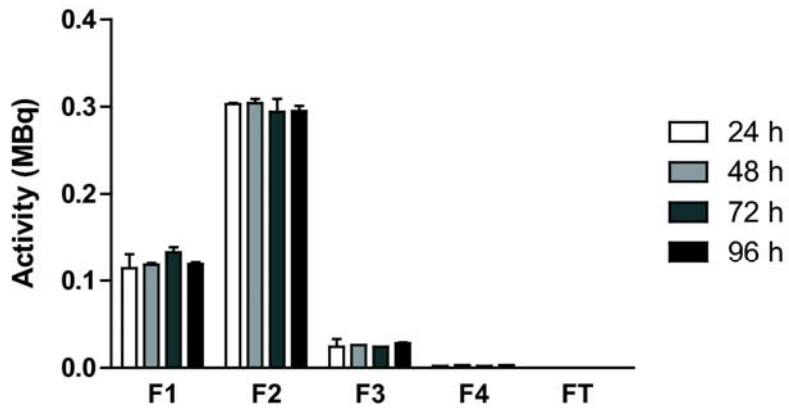
Liposomes eluted in the first fractions of the size exclusion chromatography and Supplemental Figure 5 shows that most activity (MBq) is associated with the liposomes.

### **In Vivo Stability Assay**

Biodistribution experiments (Supplemental Figure 6) showed that liposomes are cleared from the blood over time, whereas they are retained in liver and spleen, which are known to be involved in the clearance of liposomes. This data shows that most other organs show liposome-specific activity due to perfusion at 24 h, which is cleared after several days.

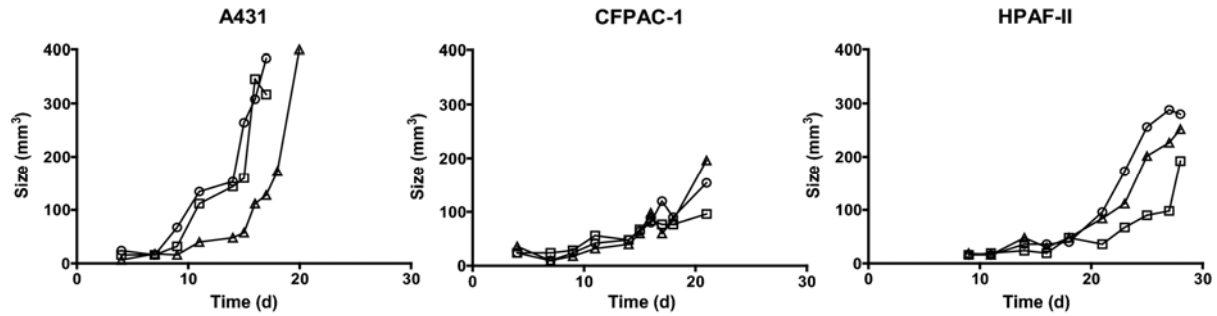
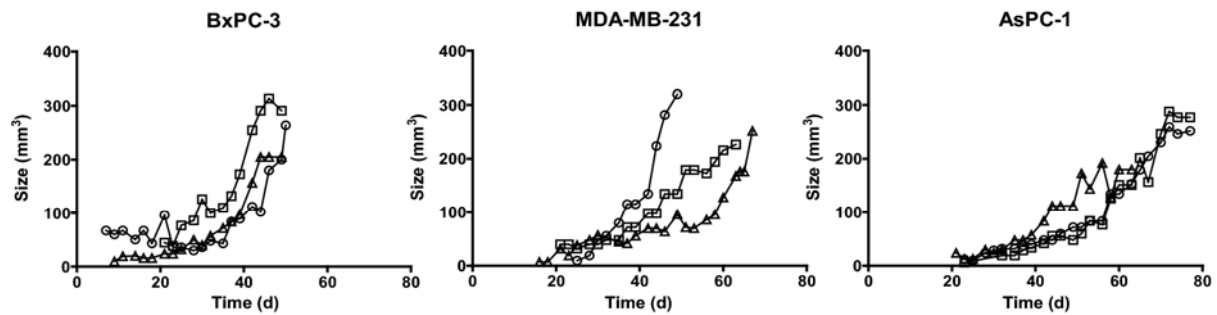
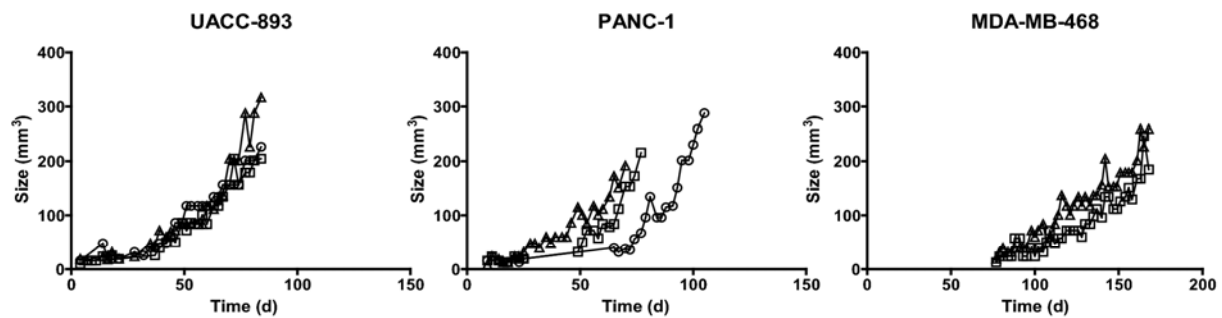
## REFERENCES

1. Lasic DD. *Liposomes from physics to applications*: Elsevier; 1993.
2. Rouser G, Fkeischer S, Yamamoto A. Two dimensional thin layer chromatographic separation of polar lipids and determination of phospholipids by phosphorus analysis of spots. *Lipids*. 1970;5:494-496.
3. Gabizon AA. Liposomal anthracyclines. *Hematol Oncol Clin North Am*. 1994;8:431-450.
4. Ranson MR, Carmichael J, O'Byrne K, Stewart S, Smith D, Howell A. Treatment of advanced breast cancer with sterically stabilized liposomal doxorubicin: results of a multicenter phase II trial. *J Clin Oncol*. 1997;15:3185-3191.
5. Muggia FM, Hainsworth JD, Jeffers S, et al. Phase II study of liposomal doxorubicin in refractory ovarian cancer: antitumor activity and toxicity modification by liposomal encapsulation. *J Clin Oncol*. 1997;15:987-993.
6. Stewart S, Jablonowski H, Goebel FD, et al. Randomized comparative trial of pegylated liposomal doxorubicin versus bleomycin and vincristine in the treatment of AIDS-related Kaposi's sarcoma. International Pegylated Liposomal Doxorubicin Study Group. *J Clin Oncol*. 1998;16:683-691.
7. Northfelt DW, Dezube BJ, Thommes JA, et al. Pegylated-liposomal doxorubicin versus doxorubicin, bleomycin, and vincristine in the treatment of AIDS-related Kaposi's sarcoma: results of a randomized phase III clinical trial. *J Clin Oncol*. 1998;16:2445-2451.



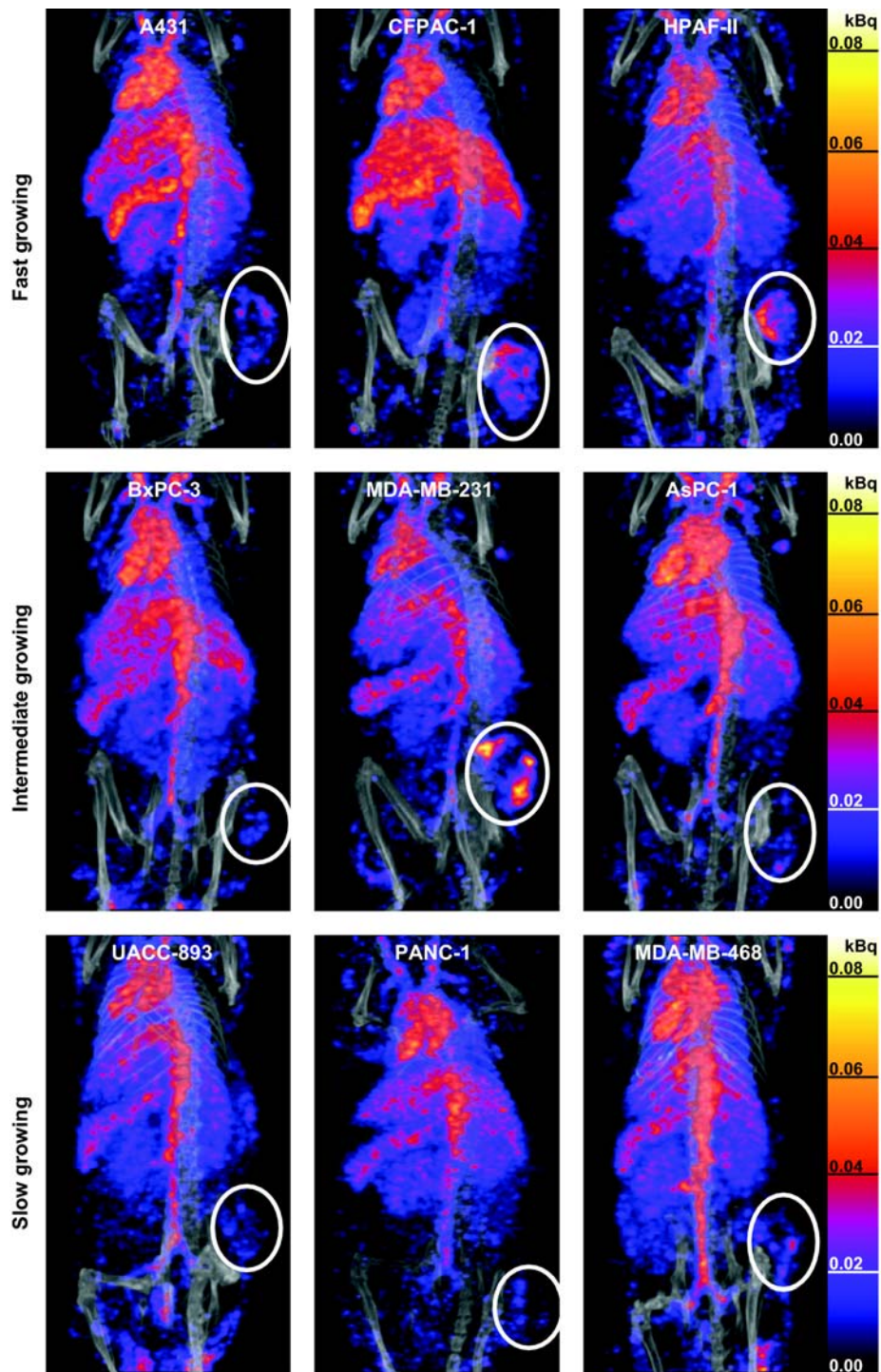
**SUPPLEMENTAL FIGURE 1.**

<sup>111</sup>In-liposomes were incubated in 100% fetal bovine serum at 37°C for t = 24, 48, 72, 96 h, after which the sample was used for size exclusion chromatography (PD-10 column). Retention activity in MBq is depicted of fractions (F1-F4 = 1 mL) collected during size exclusion chromatography and after washing the column (FT = 25 mL).

**A****B****C****SUPPLEMENTAL FIGURE 2.**

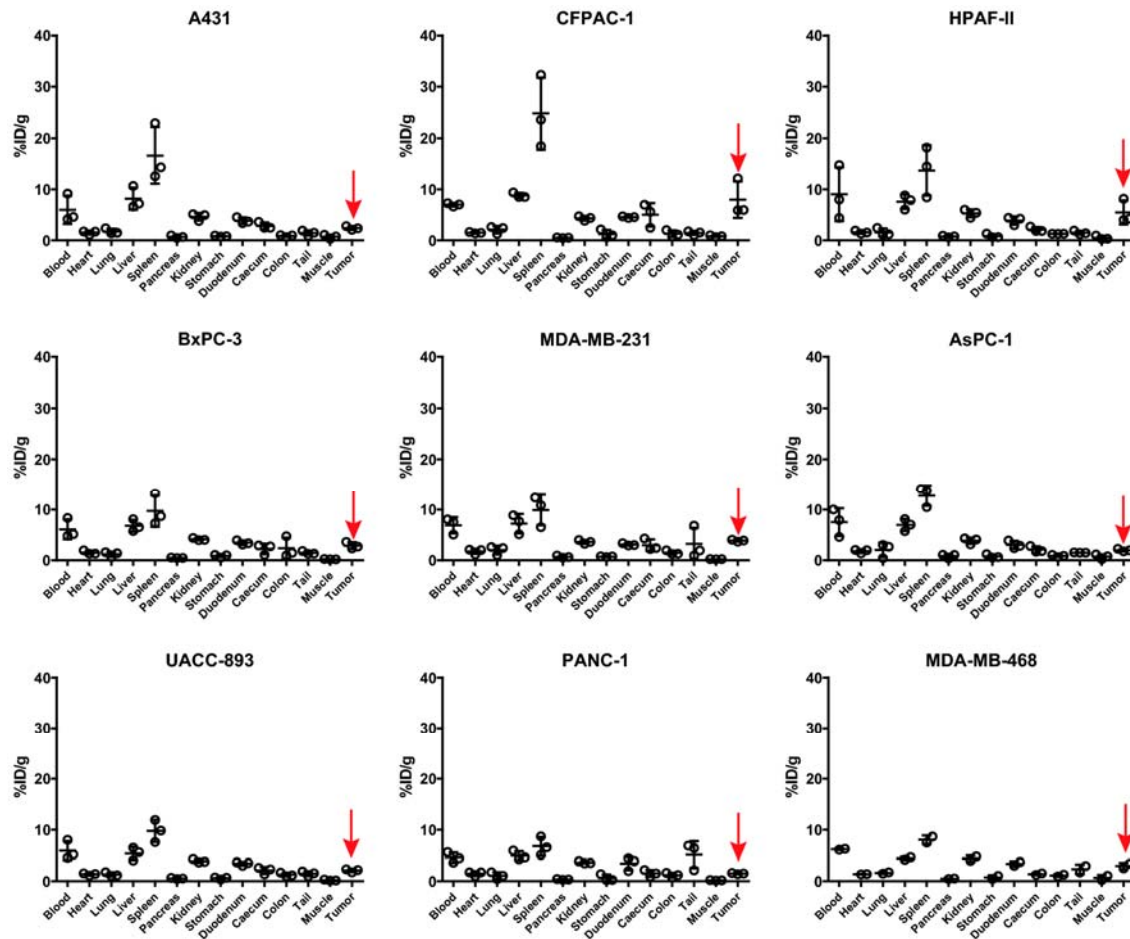
**A-C.**  $3.5 \times 10^6$  human tumor cells were inoculated s.c. in the right flank of NMRI nu/nu mice. Tumor growth was followed over time and measured three times a week. Individual mice are depicted with the following symbols: mouse 1 =  $\circ$ , mouse 2 =  $\square$ , mouse 3 =  $\Delta$ ). The tumor xenografts were ordered according to their growth *in vivo*: fast growing (**A**); intermediate growing (**B**); slow growing (**C**). Vertical axis shows tumor size (mm<sup>3</sup>); horizontal axis days after inoculation.





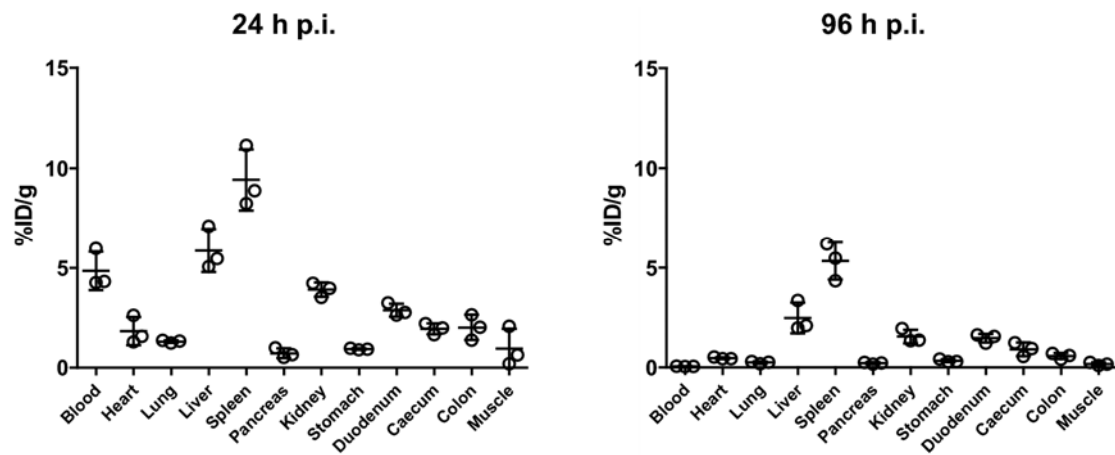
**SUPPLEMENTAL FIGURE 3.**

Representative SPECT/CT scans of fast, intermediate, and slow growing tumors 12 hours after injection. The scans have been set to the same threshold (in kBq) to compensate for  $^{111}\text{In}$  half-life. Tumors are circled in white and show uptake of liposomes to various degrees.



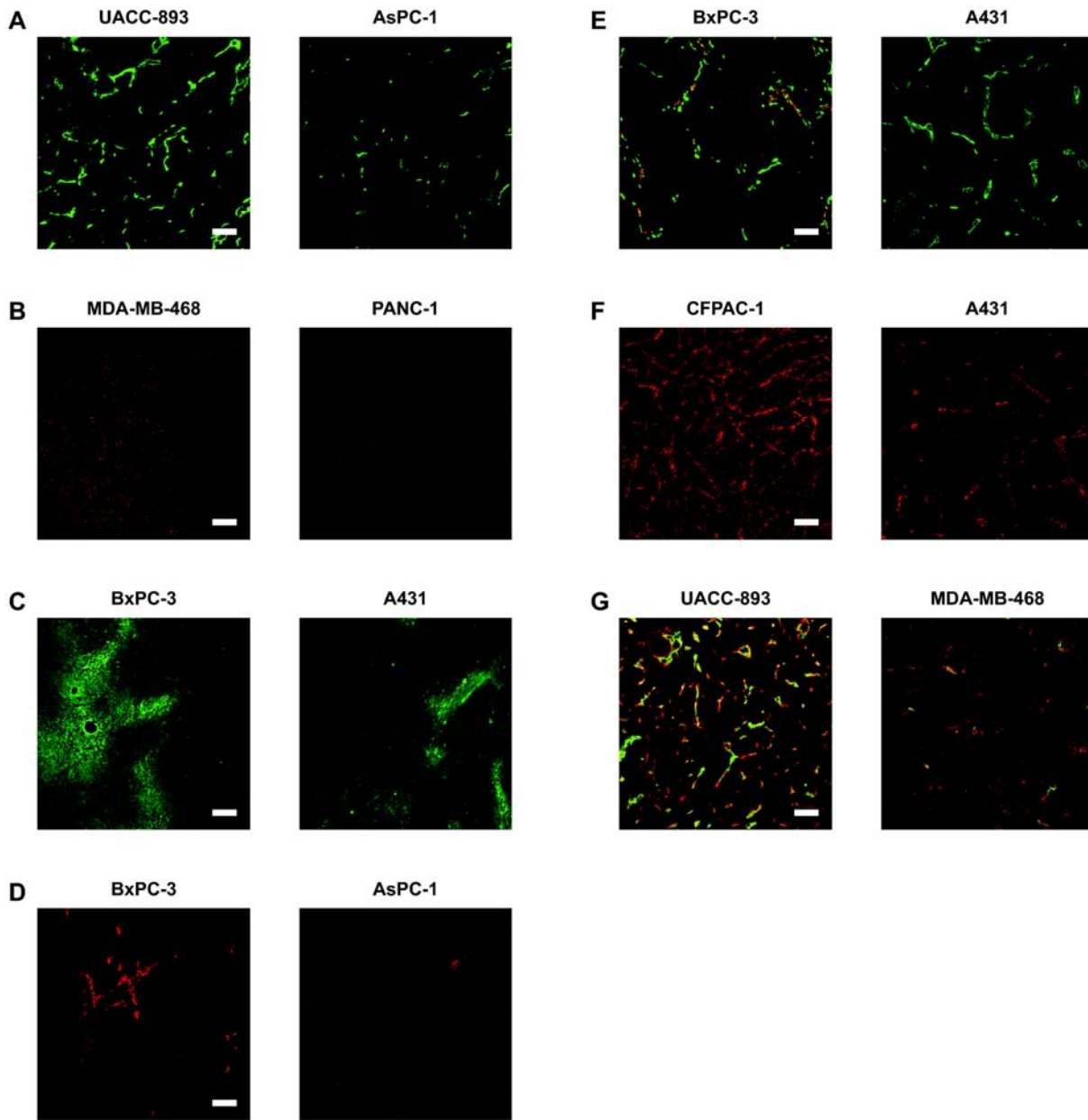
**SUPPLEMENTAL FIGURE 4.**

Percentage of injected dose per gram (%ID/g) depicted per mouse and tumor type shows a high uptake in liver, spleen, and other highly perfused tissues. Tumor measurements have been indicated by red arrow.



**SUPPLEMENTAL FIGURE 5.**

Percentage of injected dose per gram (%ID/g) depicted per mouse after biodistribution at 24 and 96 h post injection (p.i.).



**SUPPLEMENTAL FIGURE 6.**

Immunohistochemical stainings showing, **A.** Mean vessel density (MVD), **B.** Macrophage density, **C.** Hypoxia based on the presence of pimonidazole, **D.** LYVE-1 staining for lymphatic vessels, **E.** Lymphatic vessel (LYVE-1) to blood vessel (CD31) ratio, indicative of the supply and drainage of tumor tissue. **F.** Collagen IV density, **G.** Colocalization of collagen IV and blood vessels (CD31). All quantifications were performed on whole tile scans of the tumor sections. Scale bars, 100  $\mu$ m.

**SUPPLEMENTAL TABLE 1.**

		PEG %	CD31 %
PEG %	Correlation Coefficient	1.000	0.154
	p value (two-tailed)		0.454
CD31 %	Correlation Coefficient	0.154	1.000
	p value (two-tailed)	0.454	
Pimonidazole %	Correlation Coefficient	0.179	-0.123
	p value (two-tailed)	0.383	0.550
Ki67 %	Correlation Coefficient	-0.128	0.204
	p value (two-tailed)	0.534	0.317
LYVE-1 %	Correlation Coefficient	0.280	0.452
	p value (two-tailed)	0.166	0.020*
CD11b %	Correlation Coefficient	0.185	-0.060
	p value (two-tailed)	0.366	0.772
Collagen %	Correlation Coefficient	0.164	-0.142
	p value (two-tailed)	0.424	0.490
Liposomes (in vivo)	Correlation Coefficient	0.516	0.069
	p value (two-tailed)	0.007*	0.739
Liposomes (ex vivo)	Correlation Coefficient	0.623	0.065
	p value (two-tailed)	< 0.001*	0.754

Statistical test used: two-tailed Spearman's rho test

\* significant at  $p < 0.05$  level

## SUPPLEMENTAL TABLE 2.

Characteristics (median, IQR)	Fast growing xenografts (n = 9)	Intermediate growing xenografts (n = 9)	Slow growing xenografts (n = 8)	p <sup>a</sup>	p <sup>b</sup>	p <sup>c</sup>
Time in days	21 (18 - 25)	60 (44 - 67)	79 (72 - 145)	< 0.05	< 0.001	ns
Morphological parameters						
PEG percentage	4.98 (2.51 - 7.24)	3.55 (2.35 - 8.53)	2.26 (0.88 - 3.84)	ns	ns	ns
CD31 percentage	3.63 (2.56 - 4.36)	2.30 (2.06 - 4.42)	2.69 (1.85 - 5.60)	ns	ns	ns
Pimonidazole percentage	26.18 (16.32 - 37.21)	41.19 (32.28 - 47.58)	37.74 (30.09 - 44.70)	< 0.05	ns	ns
Ki67 percentage	6.10 (5.24 - 9.21)	5.55 (5.09 - 7.83)	10.36 (8.3 - 12.58)	ns	< 0.05	< 0.05
LYVE-1 percentage	0.37 (0.15 - 0.79)	0.17 (0.10 - 1.02)	0.22 (0.07 - 0.28)	ns	ns	ns
CD11b percentage	0.44 (0.28 - 1.03)	1.60 (1.23 - 2.97)	1.43 (0.27 - 3.64)	< 0.05	ns	ns
Collagen percentage	18.45 (10.84 - 19.87)	14.58 (8.36 - 16.57)	13.81 (8.88 - 19.45)	ns	ns	ns
Liposomal uptake						
Liposomes ( <i>in vivo</i> )	4.00 (2.92 - 5.01)	2.25 (1.74 - 3.77)	2.04 (1.48 - 2.25)	ns	< 0.01	ns
Liposomes ( <i>ex vivo</i> )	4.24 (2.58 - 7.06)	2.70 (2.12 - 3.79)	1.97 (1.54 - 2.48)	ns	< 0.01	ns

Abbreviations: IQR = inter quartile range, ns = not significant

Statistical test used: one-way ANOVA test, two-tailed Kruskal-Wallis test

a = fast growing versus intermediate; b = fast versus slow; c = intermediate versus slow growing